View metadata, citation and similar papers at core.ac.uk
brought to you by CORE
provided by Independent Journal of Management & Production

http://www.ijmp.jor.br v. 10, n. 8, Special Edition Seng 2019
ISSN: 2236-269X
DOI: 10.14807/ijmp.v10i8.1058

INVISTIGATING THE EFFECTS OF FRP BARS ON THE SEISMIC BEHAVIOR OF REINFORCED CONCRETE COUPLING BEAMS

Mojtaba Fallahi
Islamic Azad University of Ahar, Iran, Islamic Republic of
E-mail: m_fallahi64@yahoo.com

Sajjad Sayyar Roudsari
North Carolina A&T State University, United States
E-mail: ssayyarroudsari@aggies.ncat.edu

Taher M Abu-Lebdeh
North Carolina A&T State University, United States
E-mail: taher@ncat.edu

Florian Ion T. Petrescu
Bucharest Polytechnic University,Romania
E-mail: fitpetrescu@gmail.com

Submission: 16/05/2019
Revision: 20/05/2019
Accept: 30/07/2019

ABSTRACT

Sometimes, it is necessary to install regular openings like windows or doors in the shear walls. Such openings require special reinforcement. There are several methods for reinforcing deep beams, one of which is the use of fiber reinforced polymer bars. In this study, an experimental work on a coupled shear wall has been used to mode the system by using finite element method with ABAQUS software. The finite element model was established based on part of the experimental study and verified with the other parts of the experimental results. The comparison shows good agreement. In the study, three different types of fiber reinforced polymer bars were considered in improving the mechanical and structural behavior of RC coupling beams. Results of the finite element analysis showed the superiority of the CFRP bars in improving seismic behavior of the coupled shear wall comparing to GFRP and BFRP.

[http://creativecommons.org/licenses/by/3.0/us/]
Licensed under a Creative Commons Attribution 3.0 United States License

ISSN: 2236-269X
DOI: 10.14807/ijmp.v10i8.1058

Keywords: FRP bars ; seismic behavior; coupling beams; ABAQUS software; shear walls

1. INTRODUCTION

Reinforced concrete shear wall system is one of the most common lateral load-bearing systems. It is suitable for seismic loadings. However, it is necessary to install regular openings for windows or doors in shear walls in accordance with architectural considerations and in such cases, reinforced concrete coupling beam is used. The coupling beam, which is an important member in the performance and formation of the coupled shear walls, may be restored and strengthened for various reasons.

There are several methods for reinforcing such beams, one of which is the use of fiber reinforced polymer bars (FRP). It should be noted that FRP bars have high strength-to-weight ratio, but low elastic modulus. It has linear deformation until rupture, leading to brittle failure. Further, concrete members reinforced with FRP exhibit larger deflections and crack widths comparing to steel reinforced concrete structures (GE et al., 2019).

In recent years, several numerical and experimental studies have been conducted on coupling beams of reinforced concrete coupled shear walls. For instance, Reazpour et al. (REZAPOUR; GHASSEMIEH, 2018) used Multiple-Vertical-Line-Element-Model (MVLEM) to analyze several types of macroscopic models of coupled concrete shear walls. Their results indicated that the macroscopic wall with moderate connection stiffness has acceptable consistency in terms of static and dynamic responses of the microscopic model.

Ding et al (2018) developed an analytical model for seismic simulation of reinforced concrete coupled shear walls. They proposed new mixed beam-shell model for the seismic analysis of reinforced concrete coupled walls with sufficient efficiency and accuracy on the platform of general finite element software MSC. Marc. Faridani and Capsoni (2017) assessed coupled shear walls (CSWs) equipped with passive damping systems using the damped continuum models developed as Coupled-Two-Beams (CTB).

His work showed that the developed CTB systems with the shear damping model are suitable tools for the dynamic analysis, and for the preliminary design of

[http://creativecommons.org/licenses/by/3.0/us/]
Licensed under a Creative Commons Attribution 3.0 United States License

ISSN: 2236-269X
DOI: 10.14807/ijmp.v10i8.1058

CSWs equipped with velocity-dependent dampers. Cheng, Fikri and Chen (2015) conducted experimental investigation on two approximately half-scale four-story coupled shear wall specimens. The walls were subjected to both gravity and reversals lateral displacement. They concluded that a ductile coupling beam design does not guarantee a ductile behavior of the coupled shear wall system.

On an attempt to investigate the effect of coupled shear walls on the seismic response of tall buildings, Faridani and Capsoni (2016) investigated the effects of viscous damping mechanisms on structural characteristics in coupled shear walls. They addressed energy dissipation mechanisms to investigate the effects of the internal and external viscous damping on structural characteristics in coupled shear walls.

A discrete Reference Beam (RB) was first proposed and a Distributed Internal Viscous Damping (DIVD), composed by bending and shear mechanisms, was defined. Their results revealed that the bending and shear damping are somehow efficient where the linear classical damping is incapable to be always a proper mechanism.

Based on previous researches, several methods have been proposed to strengthen RC members. One of these methods is the attachment of advanced composites, such as glass fiber reinforced plastic (GFRP) and carbon fiber reinforced plastic (CFRP), to the tension side of the members (SU; ZHU, 2005).

Although, these composites are generally capable of increasing both the ductility and the load capacity but are prone to peeling and delamination under shear stresses and deboning under cyclic loading. On the other hand, an effective method of replacing steel bars with composite bars have shown considerable strength against corrosion. It is widely used in offshore concrete structures that exposed to salty corrosive water. Cai, Wang and Wang (2017) conducted experimental study on an innovative concrete building column which are longitudinally reinforced with both steel bars and fiber-reinforced polymer (FRP) composite bars.

Despite the various studies on evaluating the seismic behavior of RC coupling beams, there are little researches on the effect of composite bars on the seismic performance of such beams. The aim of this study is to develop a finite element

[http://creativecommons.org/licenses/by/3.0/us/]
Licensed under a Creative Commons Attribution 3.0 United States License

ISSN: 2236-269X
DOI: 10.14807/ijmp.v10i8.1058

model to investigate the effect of composite bars on the seismic performance of coupling beams in terms of ductility, stiffness and overall strength.

2. MATERIALS AND METHODS: FINITE ELEMENT MODEL DEVELOPMENT

In this study, the experimental work of Su and Zhu (2005) and Zaidi et al. (2017) were utilized to model a coupled shear wall using finite element method with ABAQUS software. The configuration of the model is illustrated in figure 1. Material properties of concrete, reinforcing steel, and fiber reinforcement polymer are shown in tables 1 and 2.

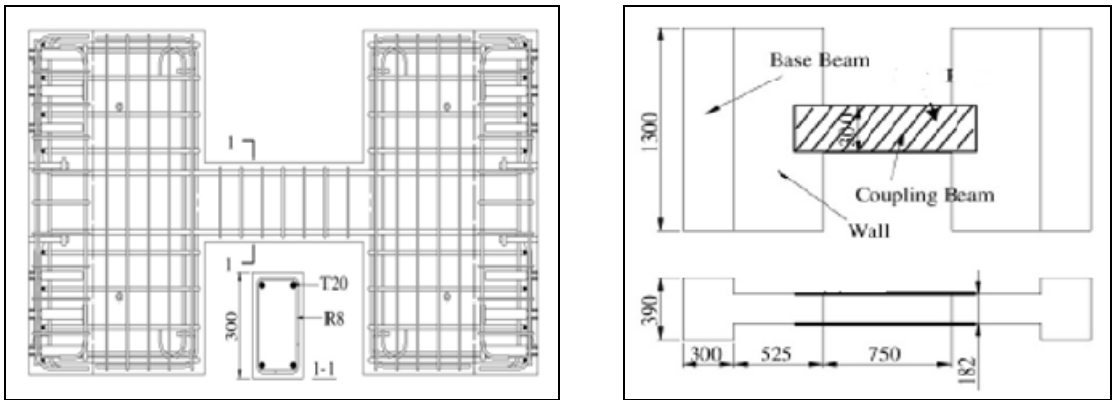

Figure 1: Configuration and reinforcement details of model (SU; ZHU, 2005)

Table 1: Material properties

Material	ID	f_{cu}	f'_c
Concrete	CB	50.2	43.9
Steel		f_y	Young's modolous
Steel bar	R8	462.7	212000
Steel bar	T10	571.0	211000
Steel bar	T12	529.3	207000
Steel bar	T16	549.2	210000
Steel bar	T20	504.1	203000

Table 2: Physical and Mechanical properties of fiber reinforcement polymer

Property	Glass Fiber	Carbon Fiber	Aramid Fiber
Elasticity modulus along Fiber (GPa)	35-60	100-580	40-125
Tensile strength (MPa)	450-1600	600-3500	1000-2500
Ultimate failure strain, %.	1.2-3.7	0.5-1.7	1.9-4.4

The ABAQUS finite element software was used in the modeling. In the modeling process, C3D8R, T3D2 and B31 element types were chosen for concrete, stirrups and longitudinal bars respectively. C3D8R (Figure 2) is a continuum element with reduced integration and hourglass control and capable of simulating concrete cracking in tension and crushing in compression.

[http://creativecommons.org/licenses/by/3.0/us/]
Licensed under a Creative Commons Attribution 3.0 United States License

ISSN: 2236-269X
DOI: 10.14807/ijmp.v10i8.1058

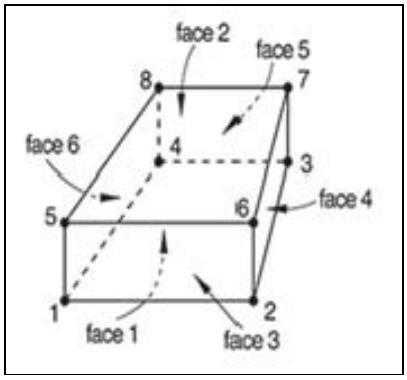

Figure 2: C3D8R element type

T3D2 is a two-node, 3-dimensional truss element used in two and three dimensions to model slender, line-like structures that support only axial loading along the element. No moments or forces perpendicular to the centerline is supported. B31 is a linear 3-dimensional beam element which does not allow for transverse shear deformation. In this element, plane sections initially normal to the beam's axis remain plane (if there is no warping) and normal to the beam axis.

The ABAQUS finite element model of the considered configuration is illustrated in figure 3. Further, in this study, concrete damage plasticity model was used to simulate concrete behavior. The material model is a continuum, plasticity based, damaged model for concrete. Damaged plasticity is assumed to characterize the uniaxial tensile and compressive response of concrete as shown in Figure 4.

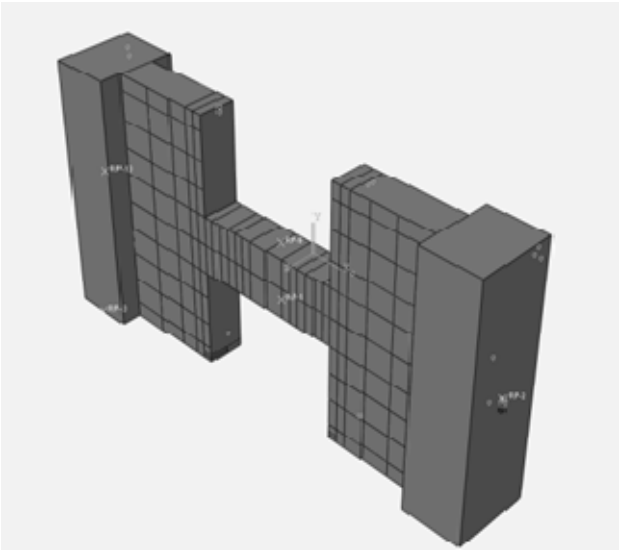

Figure 3: Finite element model

[http://creativecommons.org/licenses/by/3.0/us/]
Licensed under a Creative Commons Attribution 3.0 United States License

ISSN: 2236-269X
DOI: 10.14807/ijmp.v10i8.1058

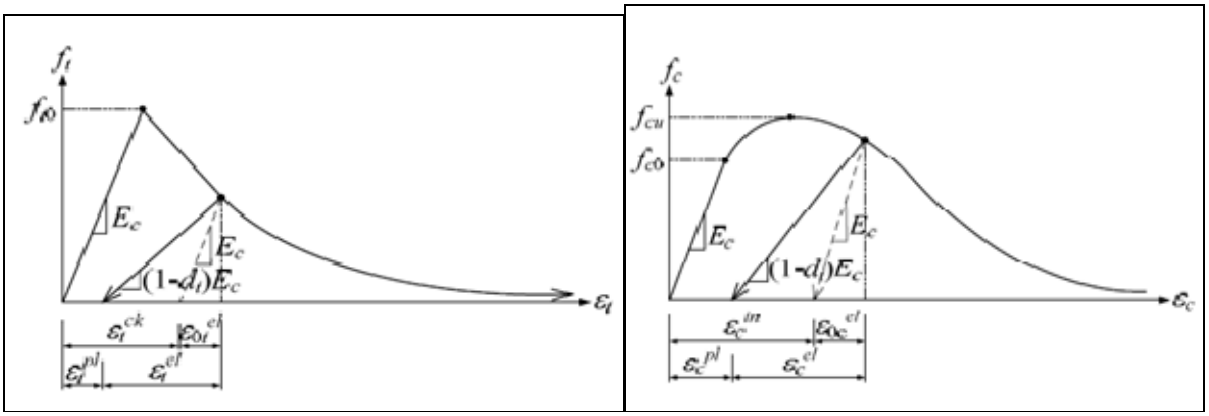

(a) (b)

Figure 4: Concrete damaged plasticity model. (a): Tension behavior associated with tension stiffening; (b): Compressive behavior associated with compression hardening
Source: ABAQUS (2014)

It is assumed that the uniaxial tension stress-strain relationship is linearly elastic until failure stress f_{t0} is reached. Beyond the state of the failure stress, the stress-strain response is designed by softening characteristic (Figure 4a). Under uniaxial compression, the response is linear up to the initial yield f_{c0}. After attaining the ultimate stress FCU in the plastic zone, the response of concrete is characterized by the stress hardening followed by strain softening (Figure 4b). Therefore, concrete stresses determined to unload from any point on the strain are:

$$f_t = E_c \cdot \left(\varepsilon_t - \varepsilon_t^{pl}\right) \cdot \left(1 - d_t\right) \quad (1)$$

$$f_c = E_c \cdot \left(\varepsilon_t - \varepsilon_t^{pl}\right) \cdot \left(1 - d_c\right) \quad (2)$$

Where E_c is the modulus of elasticity of concrete. The effective tensile and compressive cohesion stresses of concrete which determine the size of the failure surface are estimated as:

$$\bar{f}_t = \frac{f_t}{1 - d_t} = E_c \cdot \left(\varepsilon_t - \varepsilon_t^{pl}\right) \quad (3)$$

$$\bar{f}_c = \frac{f_c}{1 - d_c} = E_c \cdot \left(\varepsilon_c - \varepsilon_c^{pl}\right) \quad (4)$$

The post-failure behavior of the reinforced concrete can be expressed by means of the post-failure stress as a function of cracking strain ε_t^{ck} and ε_c^{ck} which are defined as the total strain minus the elastic strain corresponding to the undamaged material. The tension stiffening data are given in terms of the cracking strains. When

[http://creativecommons.org/licenses/by/3.0/us/]
Licensed under a Creative Commons Attribution 3.0 United States License

ISSN: 2236-269X
DOI: 10.14807/ijmp.v10i8.1058

unloading data are available, programming automatically converts the cracking strain values to plastic strain values using the following relationships (ABAQUS, 2014).

$$\varepsilon_t^{pl} = \varepsilon_t^{ck} - \frac{d_t}{1-d_t} \cdot \frac{f_t}{E_0} \quad (5)$$

$$\varepsilon_c^{pl} = \varepsilon_c^{ck} - \frac{d_c}{1-d_c} \cdot \frac{f_c}{E_0} \quad (6)$$

3. VERIFICATION OF THE PROPOSED FINITE ELEMENT MODEL

In this study, the finite element model was established based on the experimental study carried out by Su and Zhu in (2005). Figure 5 shows the test setup and loading sequence. Loading was applied by a 500 KN actuator located at the top end with the line of action passing through the beam's center. To simulate the real situation, in which the wall's piers at the two ends of a coupling beam remain parallel under deflections, a parallel mechanism was installed to connect the upper rigid arm with the lower structural steel beam fixed at the floor (SU; ZHU, 2005).

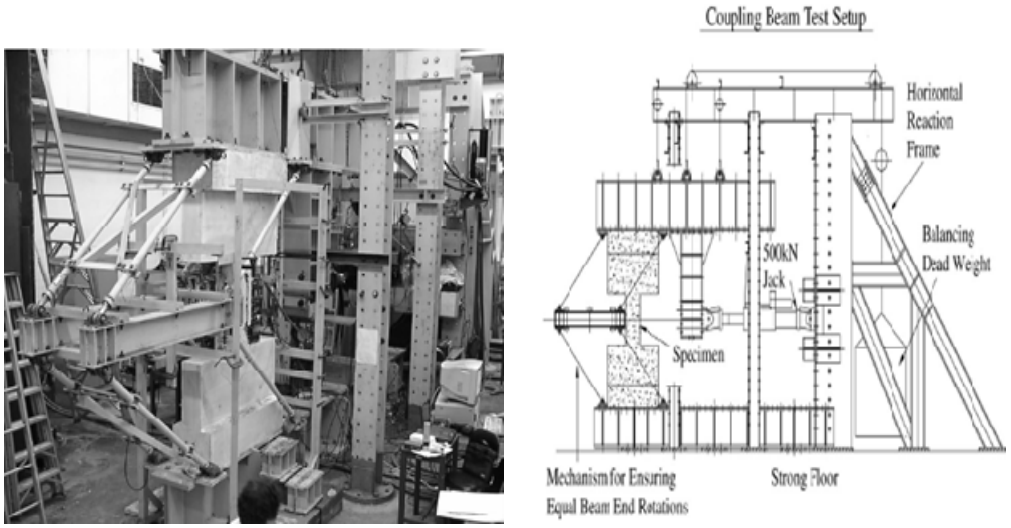

Figure 5: Test Set up
Source: Su; Zhu (2005)

The results of the finite element numerical analysis based on the above procedure are compared with the shear force-chord rotation angle of the experimental specimen and shown in Fig. 6. According to Figure 6, there is an acceptable agreement between experimental and numerical model. The proposed finite element model is capable of predicting the actual response of the structure accurately. Also, it can be seen from the curves that the numerical model is to some

[http://creativecommons.org/licenses/by/3.0/us/]
Licensed under a Creative Commons Attribution 3.0 United States License

ISSN: 2236-269X
DOI: 10.14807/ijmp.v10i8.1058

extent stiffer than the experimental model, which is an obvious consequence of the finite element method.

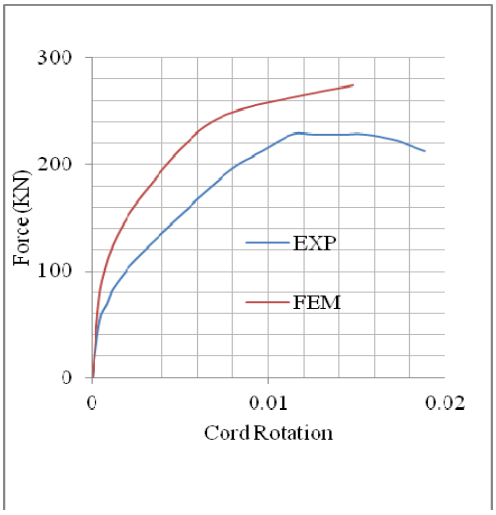

Figure 6: Comparison of shear force-chord rotation curves for experimental and numerical models

4. PRPOSED STRENGHENING METHOD AND RESULTS

Due to the brittle failure modes of concrete, various strengthening methods have been proposed by researchers. These methods can increase the ductility and seismic performance of the structures considerably. In this study, three types of fiber reinforced polymer were used to replace steel reinforcement in order to improve both the mechanical and structural behaviour of RC coupling beams.

The Physical-mechanical properties of FRP used in this study as a reinforcing material are presented in Table 2. In this study, one control model and six different finite element model have been considered based on the strengthening procedures. Table 3 shows the properties of finite element models based on strengthening method.

Table 3: Numerical Specimens Specification

SPECIMEN ID	Method of strengthening	Type of Fiber	Bar diameter (mm)
control	-	-	-
CFRP-T	Coupling beam	CFRP	20
CFRP-L	Whole model	CFRP	12,16,20
GFRP-T	Coupling beam	GFRP	20
GFRP-L	Whole model	GFRP	12,16,20
BFRP-T	Coupling beam	BFRP	20
BFRP-L	Whole model	BFRP	12,16,20

Results of the finite element analysis are presented in form of load-displacement and load-chord rotation in Figures 7 and 8. Figures 7(a) and 8 shows load-rotation and load-displacement curves for the situation in which the longitudinal

[http://creativecommons.org/licenses/by/3.0/us/]
Licensed under a Creative Commons Attribution 3.0 United States License

ISSN: 2236-269X
DOI: 10.14807/ijmp.v10i8.1058

bars of the coupling beam are replaced with glass, carbon, and aramid composite bars. It is obvious that the CFRP bars show the best ability in enhancing the load carrying capacity of the coupled shear wall comparing to FRP bars.

By contrast, the GFRP and BFRP bars cause small reduction in the load carrying capacity of the coupling beam in comparison to steel bars. The results of replacing longitudinal bars in the entire structure (coupling beam and shear wall) (Figure 7 b) is approximately similar to Figure 7 a. Comparison between equivalent plastic strain of two specimens is presented in Figure 9 (a, b).

As can be seen, the development of plastic strain in CFRP-T specimen is considerably higher than BFRP-T which this is due to better performance and efficiency of CFRP bars in comparison with BFRP (The higher the amount of yielded elements, the greater the energy dissipation of the system).

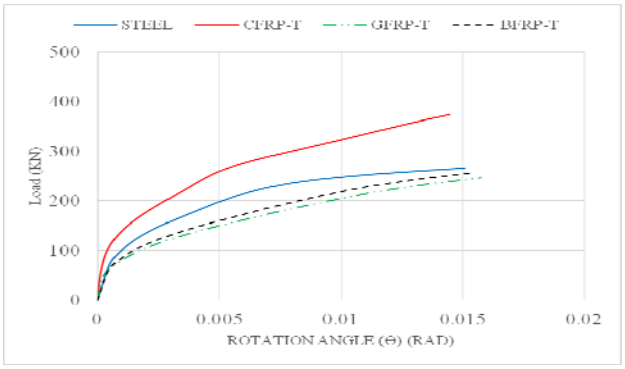

(a) Results for utilizing FRP bars in coupling beam

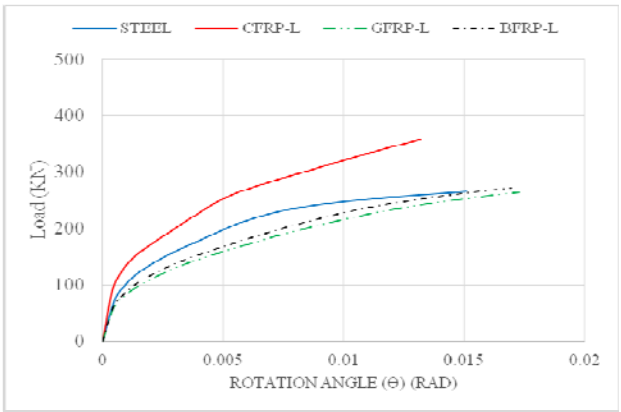

(b) Results for utilizing FRP bars in whole model

Figure 7: Comparison of FEM shear force-chord rotation curves

[http://creativecommons.org/licenses/by/3.0/us/]
Licensed under a Creative Commons Attribution 3.0 United States License

ISSN: 2236-269X
DOI: 10.14807/ijmp.v10i8.1058

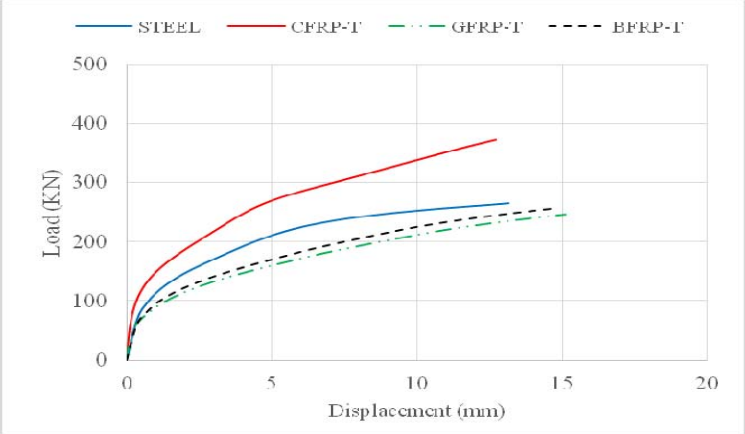

(a) results for utilizing FRP bars in coupling beam

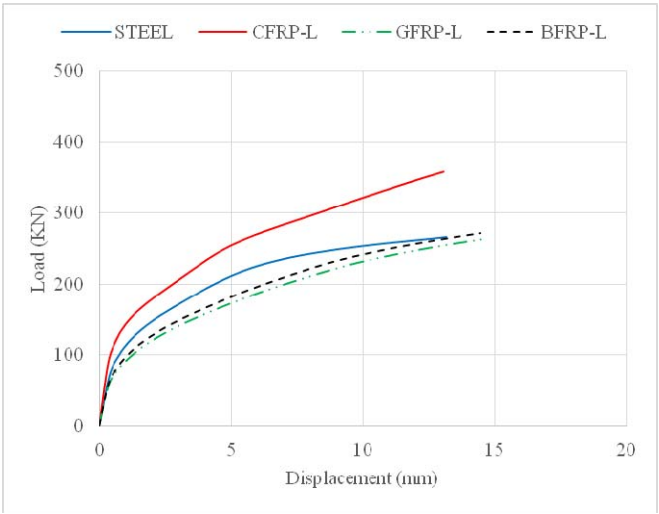

(b) results for utilizing FRP bars in whole model

Figure 8: Comparison of FEM Shear Force-Displacement Curves

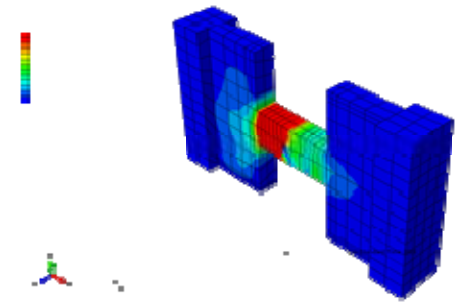

(a) equivalent plastic strain in CFRP-T

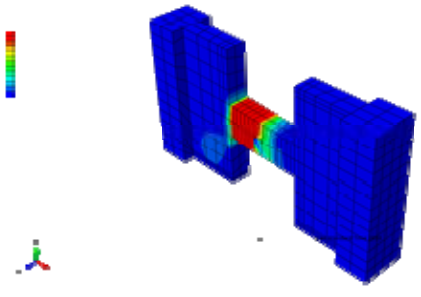

(b) equivalent plastic strain in BFRP-T

Figure 9: Comparison Between Equivalent Plastic Strain of two Specimens

5. DISCUSSION

In order to evaluate the seismic performance of the FRP coupled shear walls, parameters such as response reduction factor, ductility, energy absorption and initial

[http://creativecommons.org/licenses/by/3.0/us/]
Licensed under a Creative Commons Attribution 3.0 United States License

ISSN: 2236-269X
DOI: 10.14807/ijmp.v10i8.1058

stiffness need to be determined. In this study, the values were determined following Newmark and hall (NEWMARK; HALL, 1982).

Results of these parameters are presented later in this section. Further, it is known that the inelastic behavior of structures is usually incorporated in the design by dividing the elastic spectra by a reduction factor, R, reducing the spectrum from its original elastic demand level to a design level. Structural ductility and overstrength capacity are the crucial constituent in defining the response reduction factor. According to Patel and his co-researchers (PATEL; AMIN; PATEL, 2014), The response reduction factor can be expressed by equation 7:

$$R = R_S \cdot R_\mu \cdot R_R \tag{7}$$

In which R_S, R_μ, and R_R are the overstrength factor, ductility factor and redundancy factor respectively. According to Petrescu and his co-workers (PETRESCU et al., 2017) and Patel, Amin and Patel (2014) these reduction factors can be calculated using equation 8 and Figure 10.

$$\begin{cases} R_S = \dfrac{V_1}{V_d} \\ R_\mu = \dfrac{V_e}{V_y} \\ R_R = \dfrac{V_y}{V_1} \end{cases} \tag{8}$$

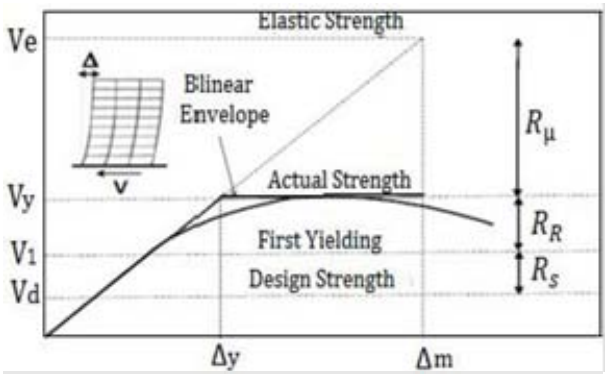

Figure 10: Bilinear curve of the response reduction factor
Source: Patel, Amin and Patel (2014)

[http://creativecommons.org/licenses/by/3.0/us/]
Licensed under a Creative Commons Attribution 3.0 United States License

ISSN: 2236-269X
DOI: 10.14807/ijmp.v10i8.1058

The initial stiffness and energy absorption can also be calculated using bilinear curves. In this study, a MATLAB code was developed to simulate the bilinear envelopes and to calculate the mentioned parameters. Figures 11 and 12 illustrate the derived bilinear envelopes of pushover curve for both steel and CFRP-L. Furthermore, values of the initial stiffness, ductility, seismic (response reduction) factor and energy absorption for all 7 specimens were calculated and the results are shown in Figures 13 to 16. It is clearly obvious from Figure 13 that CFRP-T specimen has shown the highest initial stiffness among the other specimens.

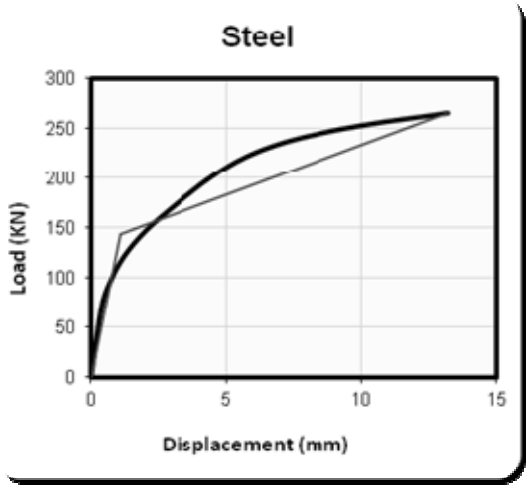

Figure 11: bilinear envelope for steel

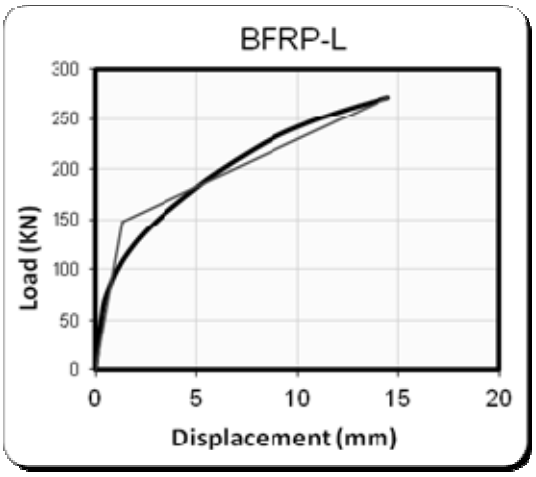

Figure 12: bilinear envelope for BFRP-L

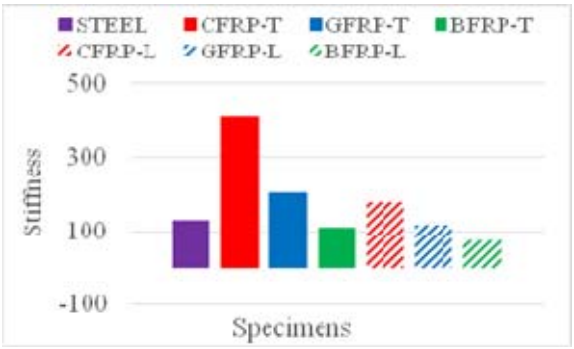

Figure 13: Comparison of initial stiffness

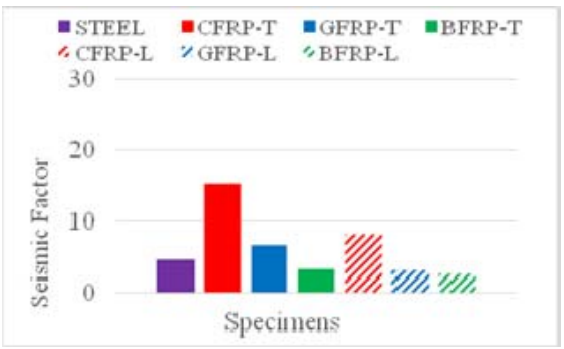

Figure 14: Comparison of a seismic factor

[http://creativecommons.org/licenses/by/3.0/us/]
Licensed under a Creative Commons Attribution 3.0 United States License

ISSN: 2236-269X
DOI: 10.14807/ijmp.v10i8.1058

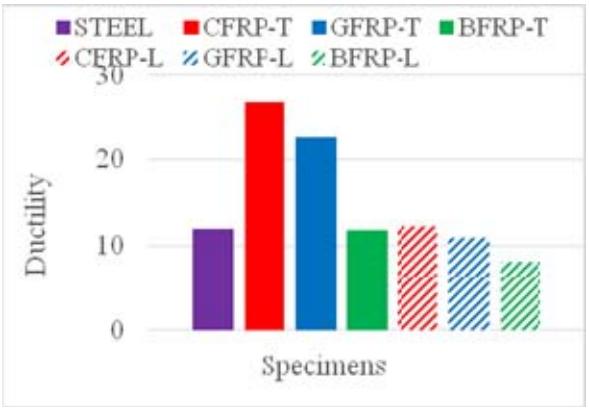

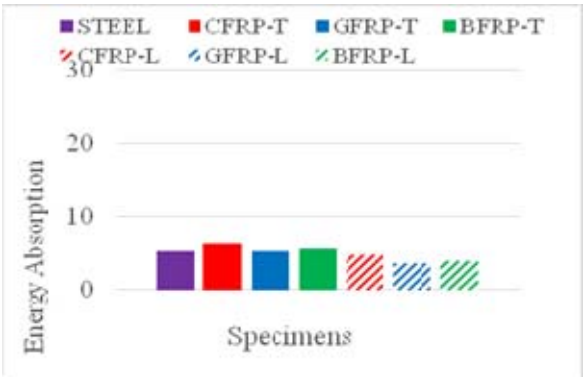

Figure 15: Comparison of ductility stiffness Figure 16: Comparison of energy absorption

As shown in the above figures, the difference between the stiffness of CFRP-T and GFRP-T is significant because. The stiffness of GFRP-T plunged to about half of its initial value. The pattern for seismic factor is approximately the same, however the maximum seismic factor is assigned to CFRP-T at 15.36, while the seismic factor of GFRP-T is 6.68 and the minimum amount has been calculated for BFRP-L at 2.67. Regarding ductility, despite the maximum obtained for CFRP-T but the difference between CFRP-T and GFRP-T decreased noteworthy. Further, the energy absorption of all specimens (Fig 15) is somehow close to each other. CFRP-T has the maximum energy absorption at 6.26E+6.

6. CONCLUSIONS

From the results obtained by the Finite Element models, the following conclusions can be drawn:

1- Comparing the results of the numerical analysis with the experimental test indicate that there is an acceptable agreement between experimental and numerical results, and thus the finite element model is capable of accurately predicting the actual response of the structure.

2. results of finite element analysis showed that FRP bars positively changed the structural response of RC coupling beams in terms of initial stiffness, ductility, and energy dissipation characteristics.

3. Comparing between the specimens in term of seismic parameters indicated that strengthening of coupling beam with FRP bars has a better seismic response than that for the whole structure.

[http://creativecommons.org/licenses/by/3.0/us/]
Licensed under a Creative Commons Attribution 3.0 United States License

ISSN: 2236-269X
DOI: 10.14807/ijmp.v10i8.1058

4. Result of the finite element analysis showed that CFRP has the highest impact in improving seismic behaviour of the coupled shear wall rather than GFRP and BFRP.

5. Based on the results, CFRP bars increased the ductility, seismic factor, stiffness, and energy absorption of the coupled shear wall by about 124%, 227%, 314%, and 18% respectively. And the results for GFRP bars is 56%, 88%, 42% and -2% respectively.

6. Unlike CFRP and GFRP, BFRP bars have some aggravating effect on the seismic performance of the wall.

REFERENCES

CAI, Z. K.; WANG, D.; WANG, Z. (2017) Full-scale seismic testing of concrete building columns reinforced with both steel and CFRP bars. **Composite Structures**, v. 178, p. 195-209

CHENG, M. Y.; FIKRI, R.; CHEN, C. C. (2015) Experimental study of reinforced concrete and hybrid coupled shear wall systems. **Engineering Structures**, v. 82, p. 214-225.

DING, R.; TAO, M. X.; NIE, X.; MO, Y. L. (2018) Analytical model for seismic simulation of reinforced concrete coupled shear walls. **Engineering Structures**, v. 168, p. 819-837.

FARIDANI, H. M.; CAPSONI, A. (2016) Investigation of the effects of viscous damping mechanisms on structural characteristics in coupled shear walls. **Engineering Structures**, v. 116, p. 121-139.

FARIDANI, H. M.; CAPSONI, A. (2017) Analysis of passively-damped coupled shear walls using continuum-based models. **Engineering Structures**, v. 148, p. 739-754.

GE, W.; ASHOUR, A. F.; CAO, D.; LU, W.; GAO, P.; YU, J.; CAI, C. (2019) Experimental study on flexural behavior of ECC-concrete composite beams reinforced with FRP bars. **Composite Structures**, v. 208, p. 454-465.

NEWMARK, N. M.; HALL, W. J. (1982) Earthquake spectra and design: **Earthquake Engineering Research Institute**. Berkeley, California.

PATEL, T.; AMIN, J.; PATEL, B. (2014) Evaluation response reduction factor of RC framed staging elevated water tank using static pushover analysis. **International Journal of Civil and Structural Engineering**, v. 4, n. 3, p. 215.

PETRESCU, R. V.; AVERSA, R.; AKASH, B., BUCINELL; R., CORCHADO, J.; BERTO, F.; MIRSAYAR, M. M.; KOSAITIS, S.; ABU-LEBDEH, T.; APICELLA, A.; PETRESCU, F. I. T. (2017) Testing by Non-Destructive Control, **American Journal of Engineering and Applied Sciences**, v. 10, n. 2, p. 568-583.

REZAPOUR, M.; GHASSEMIEH, M. (2018) Macroscopic modeling of the coupled concrete shear wall. **Engineering Structures**, v. 169, p. 37-54.

[http://creativecommons.org/licenses/by/3.0/us/]
Licensed under a Creative Commons Attribution 3.0 United States License

ISSN: 2236-269X
DOI: 10.14807/ijmp.v10i8.1058

SU, R. K. L.; ZHU, Y. (2005) Experimental and numerical studies of the external steel plate strengthened reinforced concrete coupling beams. **Engineering Structures**, v. 27, n. 10, p.1537-1550

ZAIDI, A.; BRAHIM, M. M.; MOUATTAH, K.; MASMOUDI, R. (2017). FRP Properties Effect on Numerical Deformations in FRP Bars-Reinforced Concrete Elements in Hot Zone. **Energy Procedia**, v. 139, p. 798-803

6.14 Documentation. Dassault Systemes Simulia Corporation. (2014) **ABAQUS**, 651

[http://creativecommons.org/licenses/by/3.0/us/]
Licensed under a Creative Commons Attribution 3.0 United States License